Water wave scattering by a submerged circular-arc-shaped plate

Mridula Kanoria[a], B.N. Mandal[b,*]

[a]*Department of Applied Mathematics, Calcutta University, 92 A. P. C. Road, Kolkata 700 009, India*
[b]*Physics and Applied Mathematics Unit, Indian Statistical Institute, 203, B.T. Road, Kolkata 700 108, India*

Received 21 January 2002; received in revised form 22 September 2002; accepted 28 September 2002
Communicated by S. Kida

Abstract

The problem of water wave scattering by a thin circular-arc-shaped plate submerged in infinitely deep water is investigated by linear theory. The circular-arc is not necessarily symmetric about the vertical through its center. The problem is formulated in terms of a hypersingular integral equation for a discontinuity of the potential function across the plate. The integral equation is solved approximately using a finite series involving Chebyshev polynomials of the second kind. The unknown constants in the finite series are determined numerically by using the collocation and the Galerkin methods. Both the methods ultimately produce very accurate numerical estimates for the reflection coefficient. The numerical results are depicted graphically against the wave number for a variety of configurations of the arc. Some results are compared with known results available in the literature and good agreement is achieved. The suitability of using a circular-arc-shaped plate as an element of a water wave lens has also been discussed on the basis of the present numerical results.

MSC: 76 B

Keywords: Water wave scattering; Linear theory; Circular arc; Hypersingular integral equation; Reflection coefficient

1. Introduction

A water wave lens can be constructed from a system of submerged bodies, called *elements*, to focus waves for the purpose of extracting wave energy from them (McIver and Urka, 1995). The wave focussing mechanism is similar to what governs the focussing of light waves. The system is designed in such a way that incident wave trains experience phase shifts without much reflection as

they pass over it and are transformed by the lens into converging wave trains. Thus, each element of the wave lens should be such that an incoming surface wave train experiences *little reflection* by it. It is well known that a circular cylinder with horizontal axis is transparent to normally incident waves of all frequencies when submerged in water of infinite depth (Dean, 1948; Ursell, 1950) and it can be used as an ideal element of a wave lens. However, there are some practical difficulties in using it as a lens element and other bodies such as thin horizontal plates, chevron shaped plates, etc. have been employed (McIver and Urka, 1995). McIver (1985) considered a submerged horizontal flat plate moored to the seabed to study the feasibility of its use as a lens element. There are instances of total transmission of normally incident waves past submerged obstacles at isolated frequencies. Examples of such obstacles include submerged long two-dimensional bodies, bottom mounted submerged rectangular barriers, submerged rectangular blocks (Kanoria et al., 1999), and submerged thin inclined plates (Parsons and Martin, 1992). Thus, study of water wave scattering problems involving submerged obstacles of different geometrical shapes has significant relevance in the construction of wave lens to use them as its elements. Fortunately, such study is being made in the water wave literature for the last few decades by linear theory by using a variety of mathematical techniques which essentially depend on the geometrical configurations of the obstacles. Mention may be made about the study of water wave scattering problems involving thin vertical or horizontal barriers submerged in infinitely deep or finite-depth water by many investigators (Dean 1945; Ursell, 1947; Evans, 1970; Porter, 1972; Heins, 1950; Burke, 1964; Mandal and Dolai, 1994; Porter and Evans, 1995; and others).

The case of a surface piercing thin plate inclined at an angle $\frac{(n-1)}{2n}\pi$ (n being a nonnegative integer) with the vertical was considered by John (1948) by using complex variable theory for explicit solutions. However, the method is unwieldy for $n \geqslant 2$. For arbitrary inclination of the thin plate Parsons and Martin (1992) devised a hypersingular integral equation formulation of the problem for the case when the plate is submerged in infinitely deep water to obtain very accurate numerical estimates for the reflection and transmission coefficients. The surface piercing inclined plate problem was also investigated by Parsons and Martin (1994) by the same technique with some appropriate modifications. This technique of hypersingular integral equation can also be applied for a thin curved plate and Parsons and Martin (1994) used this technique to study the case of a submerged circular-arc-shaped thin plate submerged in deep water, the plate being convex upwards and symmetric about the vertical passing through the centre of the arc. For studying the feasibility of using a circular-arc-shaped plate as a wave lens element McIver and Urka (1995) investigated the symmetric circular-arc-shaped plate problem of Parsons and Martin (1994) by two methods, one based on the method of matched series expansions and the other based on Schwinger variational approximation. They found that there is very little reflection for plates which occupy half a circle or more, and such plates are good candidates for use as lens elements.

In the present paper, we consider a submerged circular-arc-shaped plate placed arbitrarily, i.e. the plate is, in general, not symmetric with respect to the vertical through its centre and not necessarily convex upwards, and study its reflective properties for the purpose of its feasibility to use as a lens element. As in Parsons and Martin (1994), a hypersingular integral equation formulation of the problem is derived. The integral equation contains a discontinuity of the velocity potential across the plate. It is solved numerically by approximating the discontinuity in terms of a finite series involving Chebyshev polynomials of the second kind. The unknown constants appearing as coefficients in the finite series are determined numerically by using two methods. The first one is based on collocation

as has been used by Parsons and Martin (1994). The second is a Galerkin method based on utilization of the orthogonal property of the Chebyshev polynomials. Both the methods produce very accurate numerical estimates for the reflection coefficient, which are depicted graphically against the wave number for various configurations of the circular-arc plate. Some results are compared with those obtained by McIver and Urka (1995). A good agreement is seen to be achieved. When the circular-arc approaches a full circle, the reflection coefficient is almost zero, which agrees with the classical result concerning a circular cylinder mentioned above. Again, when the position of the circular-arc plate is reversed with respect to the vertical through the centre of the circle, the reflection coefficient remains unchanged. This is in accordance with the principle of complementarity theorem.

Numerical results for the reflection coefficient show that when the arc length of the plate is more than half (or less than quarter) of a circle, then its upward (or downward) convex configuration is a good candidate for use as a lens element. A semi-circular-arc-shaped plate with horizontal diameter can also be used as lens element for the low- (or high) frequency range when it is convex downward (or upward).

2. Formulation

Let a circular-arc-shaped thin plate Γ be submerged in infinitely deep water and its configuration be described by using Cartesian co-ordinates with x- and z-axis lying on the mean free surface and y-axis directed vertically downwards and passing through the centre of the circular-arc. The vertical section of the plate is in the form of an arc of a circle of radius b with centre at depth $d+b$ below the mean free surface and let α and $\beta(>\alpha)$ be the angles made with the upward vertical by the radii at two end points of the arc (see Fig. 1).

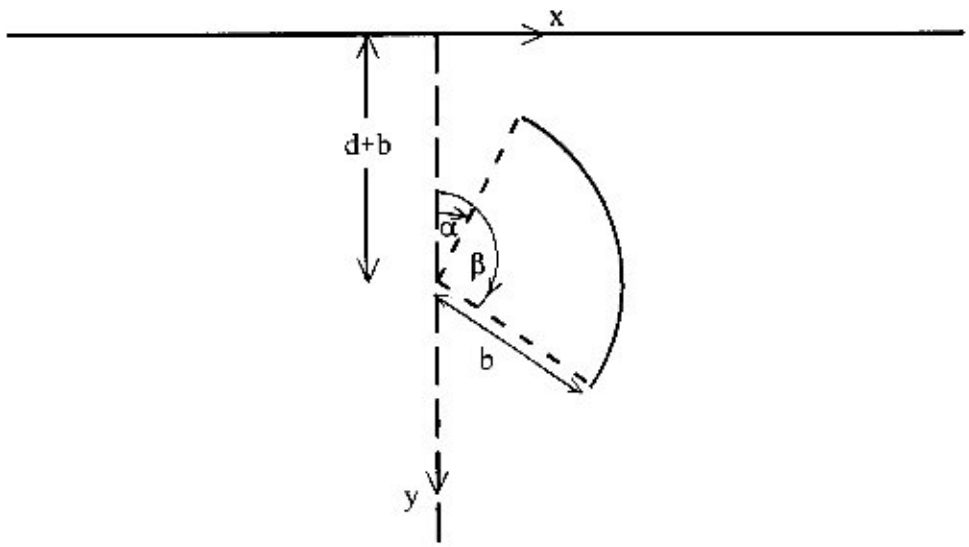

Fig. 1. Configuration of a circular-arc-shaped thin plate.

Thus, a point (x, y) on the plate Γ has the parametric representation

$$x = b\sin\Theta t, \quad y = d + b - b\cos\Theta t \left(\frac{\alpha}{\Theta} \leqslant t \leqslant \frac{\beta}{\Theta}\right),$$

where $\Theta = \beta - \alpha$.

With the usual assumptions that water waves are linear phenomena, the fluid is incompressible and inviscid, and its motion is irrotational, there exists a velocity potential which can be written as $Re\{\frac{-igb_o}{\sigma}\phi(x, y)e^{-i\sigma\tau}\}$, where b_o is the amplitude of the incoming surface wave train of angular frequency σ and described by $Re\{\frac{-igb_o}{\sigma}\phi_0(x, y)e^{-i\sigma\tau}\}$ with

$$\phi_0(x, y) = e^{-Ky+iKx}, \tag{2.1}$$

g being the acceleration due to gravity, τ the time and $K = \sigma^2/g$. It is assumed that the incoming wave train propagates along a direction normal to the axis of the cylinder whose cross section is the circle, a part of which is Γ, so that the problem is two-dimensional and independent of z. Then, the function $\phi(x, y)$ satisfies, in the fluid region, that

$$\nabla^2\phi = 0, \tag{2.2}$$

where ∇^2 is the two-dimensional Laplace operator with the free surface condition

$$K\phi + \frac{\partial\phi}{\partial y} = 0 \quad \text{on } y = 0 \tag{2.3}$$

and the condition on the plate

$$\frac{\partial\phi}{\partial n} = 0 \quad \text{on } \Gamma, \tag{2.4}$$

where $\partial/\partial n$ denotes the normal derivative at a point on Γ. The edge conditions are given by

$$r^{1/2}\nabla\phi \text{ is bounded as } r \to 0, \tag{2.5}$$

where r is the distance from the submerged edges of Γ, the infinite-depth condition by

$$\nabla\phi \to 0 \quad \text{as } y \to \infty, \tag{2.6}$$

and the condition at infinity by

$$\phi(x, y) \to \begin{cases} T\phi_0(x, y) & \text{as } x \to \infty, \\ \phi_0(x, y) + R\phi_0(-x, y) & \text{as } x \to -\infty, \end{cases} \tag{2.7}$$

where R and T denote, respectively, the reflection and transmission coefficients, and are to be determined.

3. Method of solution

In order to obtain a representation of the function $\phi(x, y)$ satisfying (2.2), (2.3), (2.6) and (2.7) we need the source potential $G(x, y; \xi, \eta)(\eta > 0)$ which satisfies

$\nabla^2 G = 0$ in the fluid region except at (ξ, η),

$$G \to \ln r \text{ as } r = \{(x-\xi)^2 + (y-\eta)^2\}^{1/2} \to 0,$$

$$KG + \frac{\partial G}{\partial y} = 0 \quad \text{on } y = 0,$$

$$\nabla G \to 0 \quad \text{as } y \to \infty,$$

$$G(x, y; \xi, \eta) \to \text{const}\, e^{-K(y+\eta)+iK|x-\xi|} \quad \text{as } |x-\xi| \to \infty.$$

Then G is given by (cf. Mandal and Chakrabarti, 2000, p. 28)

$$G(x, y; \xi, \eta) = \ln \frac{r}{r'} - 2\int_C \frac{e^{-k(y+\eta)}}{k-K} \cos k(x-\xi)\, dk, \tag{3.1}$$

where $r, r' = \{(x-\xi)^2 + (y \mp \eta)^2\}^{1/2}$, and C denotes a path along the positive real axis in the complex k-plane indented below the pole at $k = K$.

We now apply the Green integral theorem to the functions $\phi(x, y) - \phi_0(x, y)$ and $G(x, y; \xi, \eta)$ in the region bounded by the lines $y = 0$, $-X \leqslant x \leqslant X$; $x = \pm X$, $0 \leqslant y \leqslant Y$; $y = Y$, $-X \leqslant x \leqslant X$, a closed curve enclosing Γ and a circle of small radius ε with centre at (ξ, η), and ultimately make $X \to \infty$, $Y \to \infty$, and the two sides of the closed curve enclosing Γ shrinking almost to Γ and $\varepsilon \to 0$. Then, we obtain

$$\phi(\xi, \eta) = \phi_0(\xi, \eta) - \frac{1}{2\pi}\int_\Gamma F(q) \frac{\partial G}{\partial n_q}(x, y; \xi, \eta)\, ds_q, \tag{3.2}$$

where $q \equiv (x, y)$ is a point on Γ, $F(q)$ denotes the discontinuity of $\phi(x, y)$ across Γ and $\partial/\partial n_q$ the normal derivative at the point q. It should be noted that the unknown function $F(q)$ vanishes at the end points of Γ while its derivative has square root singularity there.

Use of boundary conditions (2.4) rewritten as

$$\frac{\partial \phi}{\partial n_p} = 0 \quad \text{on } \Gamma,$$

where $p \equiv (\xi, \eta)$ is another point on Γ leads to the integro-differential equation

$$\frac{\partial}{\partial n_p}\int_\Gamma F(q) \frac{\partial G}{\partial n_q}(q; p)\, ds_q = 2\pi \frac{\partial \phi_0}{\partial n_p}(\xi, \eta) \quad (p \in \Gamma), \tag{3.3}$$

where $F(q)$ vanishes at the end points of Γ. The order of differentiation and integration in (3.3) can be interchanged provided the integral is interpreted as a Hadamard finite part integral, and this leads to the hypersingular integral equation

$$\oint\!\!\!\!\!\!\times_\Gamma F(q) \frac{\partial^2 G}{\partial n_p \partial n_q}(q; p)\, ds_q = 2\pi \frac{\partial \phi_0}{\partial n_p} \quad (p \in \Gamma), \tag{3.4}$$

where the cross in the integral sign indicates a Hadamard finite part integral.

To obtain the actual expression of the kernel in (3.4), we note that the unit normals $\mathbf{n}_p$ and $\mathbf{n}_q$ at the points p and q on Γ are given by

$$\mathbf{n}_p = (\sin \Theta u, -\cos \Theta u), \quad \mathbf{n}_q = (\sin \Theta t, -\cos \Theta t), \tag{3.5}$$

where u and t denote the parametric co-ordinates of p and q, respectively. Using (3.5), we find that

$$\frac{\partial^2 G}{\partial n_p \partial n_q}(q;p) = -\frac{1}{b^2\Theta^2(u-t)^2} - \mathscr{K}(u,t) \quad \left(\frac{\alpha}{\Theta} < u,t < \frac{\beta}{\Theta}\right), \tag{3.6}$$

where

$$\begin{aligned}\mathscr{K}(u,t) = {} & \frac{1}{4b^2}\frac{1}{\sin^2\frac{\Theta}{2}(u-t)} - \frac{1}{b^2\Theta^2(u-t)^2} \\ & + \cos\Theta(u-t)\left[\frac{Y^2-X^2}{(X^2+Y^2)^2} + \frac{2KY}{(X^2+Y^2)} + 2K^2\int_C \frac{\mathrm{e}^{-kY}}{k-K}\cos kX\,\mathrm{d}k\right] \\ & + \sin\Theta(u-t)\left[\frac{2XY}{(X^2+Y^2)^2} + \frac{2KX}{(X^2+Y^2)} + 2K^2\int_C \frac{\mathrm{e}^{-kY}}{k-K}\sin kX\,\mathrm{d}k\right]\end{aligned} \tag{3.7}$$

with

$$\begin{aligned} X \equiv X(u,t) &= b(\sin\Theta t - \sin\Theta u), \\ Y \equiv Y(u,t) &= 2(d+b) - b(\cos\Theta t + \cos\Theta u). \end{aligned} \tag{3.8}$$

Following Yu and Ursell (1961), the integrals in (3.7) can be expanded as

$$\begin{aligned}\int_C \frac{\mathrm{e}^{-kY}}{k-K}\begin{pmatrix}\cos\\ \sin\end{pmatrix} kX\,\mathrm{d}k = {} & -\mathrm{e}^{KY}\left\{(\ln Kr_1 - \mathrm{i}\pi + \gamma)\begin{pmatrix}\cos\\ \sin\end{pmatrix} KX \pm \theta_1\begin{pmatrix}\sin\\ \cos\end{pmatrix} KX\right\} \\ & + \sum_{m=1}^{\infty}\frac{(-Kr_1)^m}{m!}\left(1+\frac{1}{2}+\frac{1}{3}+\cdots+\frac{1}{m}\right)\begin{pmatrix}\cos\\ -\sin\end{pmatrix} m\theta_1,\end{aligned} \tag{3.9}$$

where $\gamma = 0.5772\ldots$ is Euler's constant, $r_1 = (X^2+Y^2)^{1/2}$ and $\theta_1 = \tan^{-1}(X/Y)$.

Also, the right-hand side of (3.4) can be expressed as

$$2\pi\frac{\partial\phi_0}{\partial n_p}(p) = \frac{2\pi\mathrm{i}gb_0}{\sigma}h(u) \quad \left(\frac{\alpha}{\Theta} < u < \frac{\beta}{\Theta}\right), \tag{3.10}$$

where

$$h(u) = -K\mathrm{e}^{-K\eta(u)+\mathrm{i}K(\xi(u)+\Theta u)}.$$

Thus, (3.4) becomes

$$\text{⨍}\!\!\!\!\!-_{\alpha/\Theta}^{\beta/\Theta} g_0(t)\left[\frac{1}{(u-t)^2} + b^2\Theta^2\mathscr{K}(u,t)\right]\mathrm{d}t = -2\pi b^2\Theta^2 h(u) \quad \left(\frac{\alpha}{\Theta} < u < \frac{\beta}{\Theta}\right), \tag{3.11}$$

where

$$g_0(t) = -\frac{\sigma}{\mathrm{i}gb_0}F(t) \tag{3.12}$$

so that $g_0(t)$ may vanish at the end points $t = \alpha/\Theta, \beta/\Theta$ of the interval $(\alpha/\Theta, \beta/\Theta)$.

Replacing t and u by

$$\frac{1}{2}\left(\frac{\alpha+\beta}{\Theta}+t\right) \quad \text{and} \quad \frac{1}{2}\left(\frac{\alpha+\beta}{\Theta}+u\right)$$

respectively, we can reduce (3.11) to the hypersingular integral equation of standard form in the interval $(-1,1)$ as

$$\oint_{-1}^{1} g_1(t)\left[\frac{1}{(u-t)^2}+\mathscr{K}_1(u,t)\right]\mathrm{d}t = h_1(u)\ (-1<u<1), \tag{3.13}$$

where

$$\mathscr{K}_1(u,t)=\frac{1}{4}b^2\Theta^2\mathscr{K}\left(\frac{\alpha+\beta}{2\Theta}+\frac{u}{2},\frac{\alpha+\beta}{2\Theta}+\frac{t}{2}\right),$$

$$g_1(t)=g_0\left(\frac{\alpha+\beta}{2\Theta}+\frac{t}{2}\right),$$

$$h_1(u)=-\pi b^2\Theta^2 h\left(\frac{\alpha+\beta}{2\Theta}+\frac{u}{2}\right), \tag{3.14}$$

and $g_1(t)$ satisfies the end conditions

$$g_1(\pm 1)=0. \tag{3.15}$$

To solve (3.13) we approximate $g_1(t)$ as

$$g_1(t)=(1-t^2)^{1/2}\sum_{n=0}^{N}a_n U_n(t), \tag{3.16}$$

where N is an integer, $U_n(t)$ is the nth order Chebyshev polynomial of the second kind, and a_n $(n=0,1,\ldots,N)$ are unknown complex constants. The square root factor in (3.16) ensures that $g_1(t)$, or rather $F(q)$, has the correct behaviour at the ends of the plate. The unknown constants $a_n(n=0,1,\ldots,N)$ will be determined by using the collocation and the Galerkin methods.

Substitution of (3.16) into (3.13) leads to

$$\sum_{n=0}^{N}a_n A_n(u)=h_1(u)\quad(-1<u<1), \tag{3.17}$$

where

$$A_n(u)=-\pi(n+1)U_n(u)+\int_{-1}^{1}(1-t^2)^{1/2}\mathscr{K}_1(u,t)U_n(t)\,\mathrm{d}t. \tag{3.18}$$

The collocation points are chosen as

$$u_j=\cos\frac{j+1}{N+2}\pi\quad(j=0,1,\ldots,N). \tag{3.19}$$

Putting $u=u_j$ $(j=0,1,\ldots,N)$ in (3.17), we obtain a system of linear equations,

$$\sum_{n=0}^{N}a_n A_n(u_j)=h_1(u_j)\quad(j=0,1,\ldots,N) \tag{3.20}$$

for the determination of the constants a_n $(n=0,1,\ldots,N)$. We use the Gauss Jordan method to solve (3.20) numerically.

The orthogonal properties of the Chebyshev polynomials are used in the Galerkin method. We multiply both sides of (3.17) by $(1-u^2)^{1/2}U_m(u)$ $(m=0,1,\ldots,N)$ and integrate with respect to u over -1 to 1 to obtain another system of linear equations

$$\sum_{n=0}^{N} a_n P_{nm} = d_m \quad (m=0,1,\ldots,N), \tag{3.21}$$

where

$$P_{nm} = -\frac{\pi^2}{2}(n+1)\delta_{nm} + \int_{-1}^{1}(1-u^2)^{1/2}U_m(u)\left\{\int_{-1}^{1}\mathscr{K}_1(u,t)(1-t^2)^{1/2}U_m(t)\,\mathrm{d}t\right\}\mathrm{d}u$$

and

$$d_m = \int_{-1}^{1}(1-u^2)^{1/2}U_m(u)h_1(u)\,\mathrm{d}u. \tag{3.22}$$

Linear equations (3.21) are also solved by the Gauss Jordan method.

Now the reflection and transmission coefficients R and T are obtained by taking the limits $\xi \to \mp\infty$ in (3.2) for $\phi(\xi,\eta)$. For this purpose, we require the asymptotic result (see Mandal and Chakrabarti, 2000, p. 28)

$$G(x,y;\xi,\eta) \to -2\pi\mathrm{i}\mathrm{e}^{-K(y+\eta)\pm\mathrm{i}K(\xi-x)} \quad \text{as } \xi \to \pm\infty. \tag{3.23}$$

Making $\xi \to -\infty$ in (3.2) after using (3.23) and noting (2.7) with (x,y) replaced by (ξ,η), we find that

$$\begin{aligned} R &= \mathrm{i}K\int_{\Gamma} g_0(q)\mathrm{e}^{-Ky+\mathrm{i}Kx+\mathrm{i}\Theta t}\,\mathrm{d}s_q \\ &= \frac{\mathrm{i}Kb\Theta}{2}\sum_{n=0}^{N} a_n \int_{-1}^{1}(1-t^2)^{1/2}U_n(t)\mathrm{e}^{-K(b+d-b\cos\Theta t')+\mathrm{i}(Kb\sin\Theta+\Theta t')}\,\mathrm{d}t, \end{aligned} \tag{3.24}$$

with $t' = (\alpha+\beta)/2\Theta + t/2$. Similarly, the limit $\xi \to \infty$ leads to

$$T = 1 + \frac{\mathrm{i}Kb\Theta}{2}\sum_{n=0}^{N} a_n \int_{-1}^{1}(1-t^2)^{1/2}U_n(t)\mathrm{e}^{-K(b+d-b\cos\Theta t')-\mathrm{i}(Kb\sin\Theta+\Theta t')}\,\mathrm{d}t. \tag{3.25}$$

Thus, once a_n $(n=0,1,\ldots,N)$ are found numerically by solving linear system (3.20) or (3.21), $|R|$ and $|T|$ can be computed from (3.24) and (3.25), respectively. Here, the integrals in (3.24) and (3.25) are evaluated numerically by Gauss quadrature. The relation

$$|R|^2 + |T|^2 = 1 \tag{3.26}$$

is used as a partial check on the correctness of the numerical results.

4. Numerical results

For a particular set of values of the depth parameter $d/b = 0.1$, wave number $Kb = 0.2$ and angles $\alpha = \pi/4, \beta = 3\pi/2$, the numerical results of $|R|$ are compared for different values of the truncation

Table 1
Reflection coefficient $|R|$ $(d/b = 0.1, \alpha = \pi/4, \beta = 3\pi/2; Kb = 0.2)$

N	Collocation method	Galerkin method
0	0.24096	0.18433
1	0.13232	0.12150
2	0.12353	0.12612
3	0.12644	0.12627
4	0.12636	0.12634
5	0.12633	
6	0.12634	
7	0.12634	

Table 2
Reflection and transmission coefficient $|R|$ and $|T|$ $(d/b = 0.1, \alpha = \pi/6, \beta = \pi/2)$

Kb	$\lvert R\rvert$	$\lvert T\rvert$	$\lvert R\rvert^2 + \lvert T\rvert^2$
1.0	0.25213	0.96769	1.00000
1.6	0.26491	0.96536	1.00000
2.2	0.22521	0.97431	1.00000

size N between the Galerkin and the collocation methods in Table 1. It is seen that slightly smaller N is sufficient for the Galerkin method compared to the collocation method to obtain numerical estimates for $|R|$ correct upto 4–5 decimal places. However, more computational time is needed for the Galerkin method compared to the collocation method because we have to compute a double integral at every stage in the former while a single integral in the latter. Thus the collocation method is advantageous. The Galerkin method may be used to check the correctness of the results computed by using the collocation method. It should be mentioned here that the truncation size N which gives the same accuracy is different depending upon the arc length, depth parameter and the wave number. For all the data presented here, N is chosen in such a way that the result is correct upto 4–5 decimal places.

Table 2 shows a representative set of values of $|R|, |T|$ and $|R|^2 + |T|^2$ for $\alpha = \pi/6, \beta = \pi/2, d/b = 0.1$ and for three different values of Kb. It is observed that relation (3.26) is satisfied upto 5 decimal places.

Since the main concern here is the reflective properties of the submerged circular-arc-shaped plate for an incoming wave train, we depict $|R|$ against the wave number for various configurations of the plate. For each data point used in the plots of various graphs for $|R|$, the transmission coefficient $|T|$ is computed so as to ensure energy equality (3.26). To visualize the dependence of the depth of submergence of the plate, the reflection coefficient $|R|$ is depicted in Fig. 2 against the wave number Kb for $\alpha = 45°, \beta = 180°$ and the depth parameter $d/b = 0.1, 0.3, 0.5$. It is observed that for a fixed wave number, $|R|$ decreases as d/b increases, i.e. the more is the depth of the submergence of the plate below the free surface the less is the reflection. This is plausible since less energy is reflected by the plate if it is submerged more below the free surface.

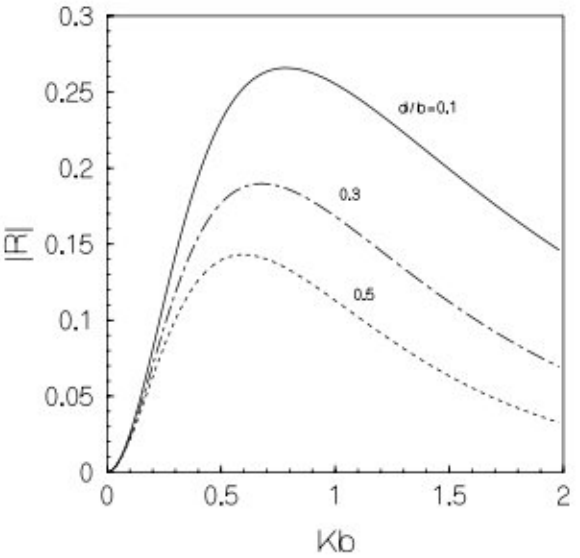

Fig. 2. Reflection coefficient vs. wave number, $\alpha = 45°, \beta = 180°$.

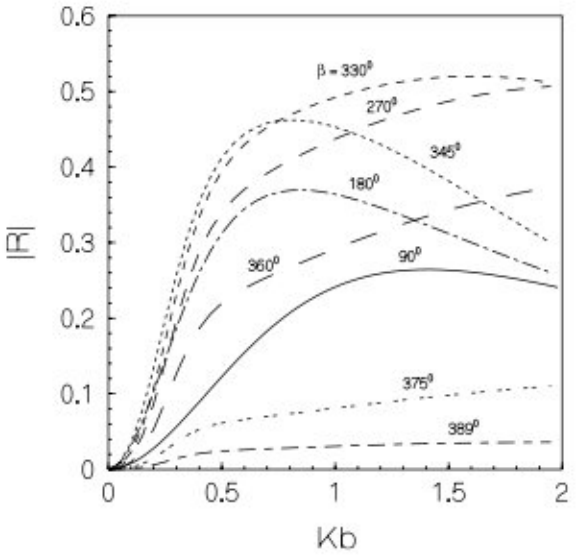

Fig. 3. Reflection coefficient vs. wave number, $d/b = 0.1, \alpha = 30°$.

Again, to visualize the effect of the arc length of the plate, $|R|$ is plotted in Fig. 3 against Kb for a number of plates whose one end is kept fixed at $\alpha = 30°$ and its centre is kept at a fixed depth ($d/b = 0.1$). The arc lengths of the plates are taken as $\beta = 90°, 180°, 270°, 330°, 345°, 360°, 375°$ and $389°$. As the arc length increases, the overall reflection coefficient initially increases (from $\beta = 90°$ to $270°$ here), takes a maximum around $\beta = 330°$ and then decreases. For the case of an almost

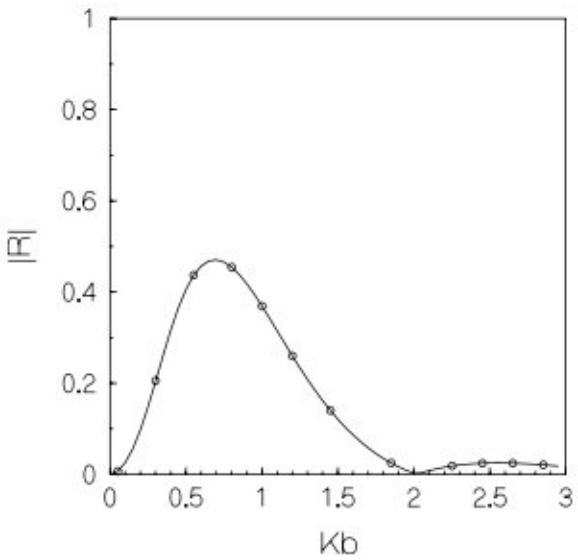

Fig. 4. Reflection coefficient vs. wave number, $d/b = 0.25$ $\alpha = -54°, \beta = 54°$, - -, present: 0, McIver and Urka (1995).

full circle ($\alpha = 30°, \beta = 389°$), the reflection is seen to be quite insignificant for all wave numbers. This is in conformity with the classical result that a long horizontal circular cylinder submerged in deep water experiences no reflection when an incoming wave train is normally incident on it. This may also be regarded as another partial check on the correctness of the numerical method employed here.

For the purpose of comparison with the results obtained by the present method and those obtained by McIver and Urka (1995) by employing the method of matched series solutions, $|R|$ is depicted in Fig. 4 for the symmetric configuration of the plate by choosing $d/b = 0.25$ and $\alpha = -54°, \beta = 54°$. The solid curve displays the present results and the circles the ones estimated from the Fig. 3 in McIver and Urka (1995). The agreement between the two is excellent. However, some differences are observed if our results are compared with theirs obtained by using the method of variational approximation and given also in Fig. 3 there (not shown here). This difference may be attributed to the fact that the method of variational approximation produces good results only when the arc length of the plate is shorter than the wavelength and the plate occupies a small fraction of a circle. It should also be noted that the method of matched series expansion employed by them produces accurate results but quite a large number of multipole potential functions are needed, e.g. 256 multipole potentials are required to ensure numerical accuracy to two decimal places. In contrast, the present method usually requires only 8–12 terms in the truncated series expansion (3.16) to get numerical accuracy upto 4–5 decimal places.

Fig. 5 depicts $|R|$ against Kb for a number of configurations of the circular-arc plate. Some configurations are symmetric and some are not, but the depth parameter $d/b = 0.1$ is common to all of them. The curve denoted by I shows $|R|$ for an upward convex symmetric circular-arc in the form of a quarter of a circle ($\alpha = -45°, \beta = 45°$) while the curve denoted by II its reflection about the horizontal diameter of the circle ($\alpha = 135°, \beta = 225°$). It is observed by comparing these two curves

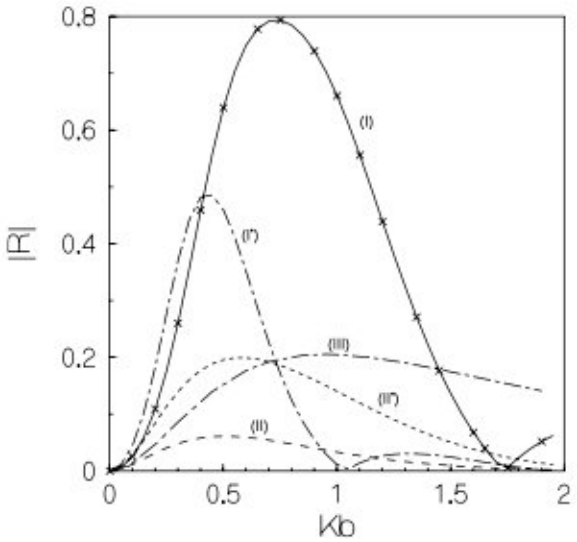

Fig. 5. Reflection coefficient vs. wave number, d/b=0.1, (1) α=−45°, β=45°, (I′) α=−80°, β=80°, (II) α=135°, β=225°, (II′) $\alpha = 100°, \beta = 260°$, (III) $\alpha = 45°, \beta = 135°$; $\alpha = 225°, \beta = 315°$, × estimated from Parsons and Martin for case (I).

that a symmetric upward convex circular-arc produces more reflection compared to a symmetric downward convex circular-arc of the same arc length and having the same centre. This is expected since the downward convex arc lying below the upward convex arc encounters less disturbances due to the incident surface wave train. The curve I′ and II′ represent $|R|$ for a symmetric upward convex circular-arc plate of arc length greater than the quarter circle but less than the half circle ($\alpha = -80°, \beta = 80°$) and its reflection about the horizontal diameter ($\alpha = 100°, \beta = 260°$). For these plates also, the upward convex arc produces more reflection compared to the downward convex arc. Curve III depicts $|R|$ for a circular-arc which is convex towards positive x direction as well as symmetric about a horizontal line passing through its centre ($\alpha = 45°, \beta = 135°$). The reversal of the position of this arc with respect to the vertical through its centre ($\alpha = 225°, \beta = 315°$) produces the same curve III. The same is true for an arc which is almost a full circle with a small opening facing an incoming wave train ($\alpha = -89°, \beta = 269°$) and for the reversed arc ($\alpha = 89°, \beta = -269°$). In this case, the curves for $|R|$ are very small for all wave numbers. This phenomenon follows from the so-called complementarity theorem which states that if the scattering body is reversed but the incident field is left unchanged, then the magnitudes of the reflection and transmission coefficients are unaltered.

Fig. 6a shows six different shapes of the circular-arc-shaped plate corresponding to (I) α=−45°, β=45°; (II) $\alpha = 45°, \beta = 315°$; (III) $\alpha = 15°, \beta = 105°$; (IV) $\alpha = -135°, \beta = 135°$; (V) $\alpha = 105°, \beta = 195°$ and (VI) $\alpha = 135°, \beta = 225°$. Fig. 6b displays $|R|$ against Kb for the shapes (I) to (VI), shown in Fig. 6a, with the same depth parameter $d/b = 0.2$. It is observed that the reflection is much reduced when the arc is convex upward compared to the case when it is convex downward and the plate length is more than half a circle. For plates occupying less than half a circle, on the other hand, the downward convex plate produces less reflection compared to the upward convex plate with the same arc length. Thus circular-arc plates occupying more than half a circle are good

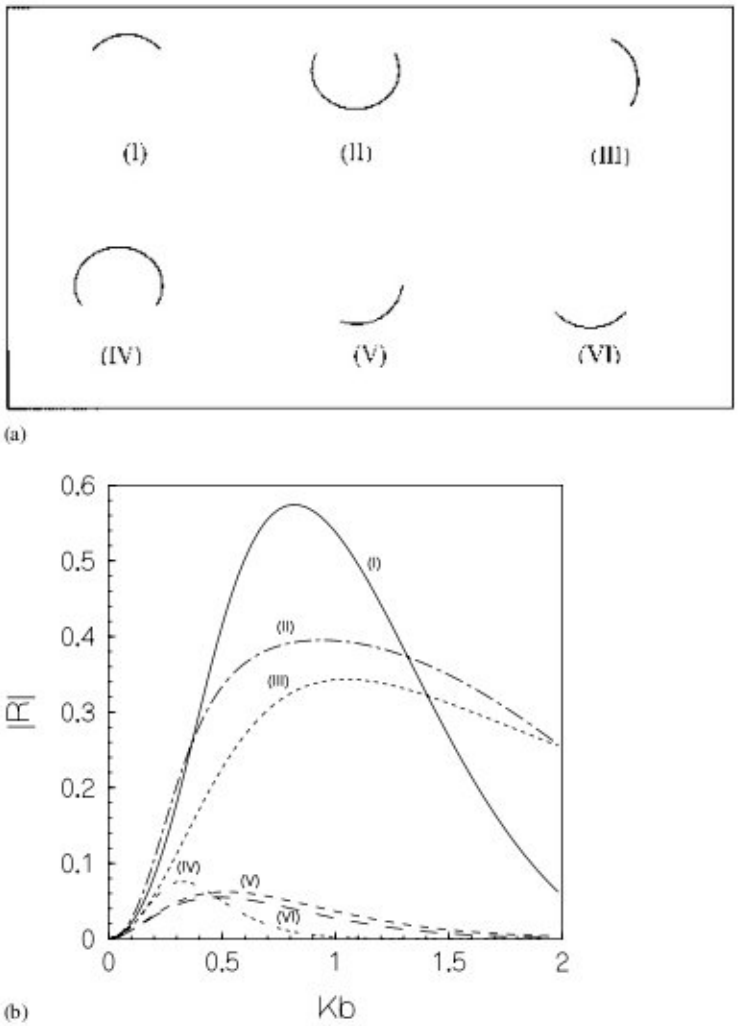

Fig. 6. (a) Different shapes of the circular-arc-shaped plate. (α,β): (I) $(-45^\circ, 45^\circ)$, (II) $(45^\circ, 315^\circ)$, (III) $(15^\circ, 105^\circ)$, (IV) $(-135^\circ, 135^\circ)$, (V) $(105^\circ, 195^\circ)$, (VI) $135^\circ, 225^\circ$; (b) Reflection coefficient vs. wave number, $d/b = 0.2$, shapes (I)–(IV).

candidates for use as elements for a water wave lens when they are convex upward. This has also been confirmed by McIver and Urka (1995) for symmetric arcs. However, circular-arc plates occupying less than half a circle and are convex downward, are also good candidates for use as lens elements. Fig. 7 depicts $|R|$ for two semi-circular-arcs with horizontal diameter, one is convex upward ($\alpha = -90^\circ, \beta = 90^\circ$) and the other is convex downward ($\alpha = 90^\circ, \beta = 270^\circ$) for $d/b = 0.2$. It is observed that the upward convex semi-circular plate produces more reflection in the low-frequency range and less reflection in the complementary range compared to the downward convex semi-circular plate. Thus their use as lens elements is dependent on the frequency range of the incoming wave train.

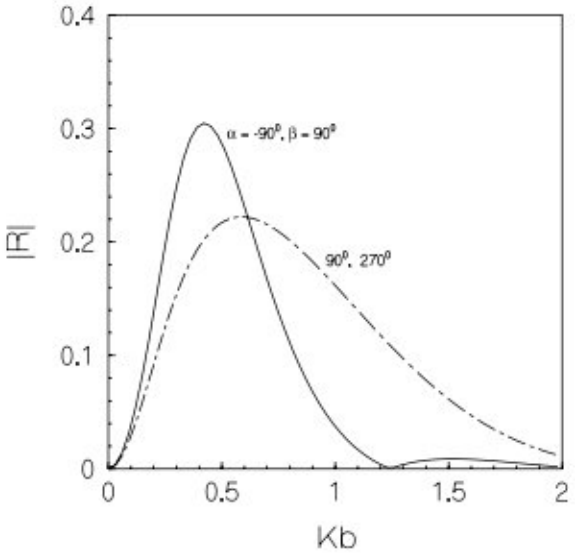

Fig. 7. Reflection coefficient vs. wave number, $d/b = 0.2$.

5. Conclusion

The reflective properties of a circular-arc-shaped thin plate submerged in deep water due to the incidence of a surface wave train are investigated here. A hypersingular integral equation formulation involving a discontinuity of the potential function across the curve plate is employed. The integral equation is solved approximately using finite series involving Chebyshev polynomials of the second kind. The collocation and Galerkin methods are used to obtain unknown constants of the finite series. Both the methods lead to very accurate numerical estimates for the reflection and transmission coefficients. Numerical results for the reflection coefficient are depicted graphically for a number of configurations of the circular-arc plate. For almost full circle the reflection coefficient is seen to be almost zero for all wave numbers, which is consistent with the classical result that a long horizontal circular cylinder submerged in deep water experiences no reflection for a normally incident train of surface water waves.

For the purpose of using a circular-arc-shaped plate as an element of a wave lens, some optimum configurations of the plate, for which the reflection coefficients remain small for all wave numbers, are inferred from the graphs for $|R|$ presented here. It is observed that the upward convex circular-arc plates experience very little reflection compared to the downward convex plates of same arc length and same depth of their centre if their arc length is more than half a circle, and are thus good candidates to be used as elements in the construction of a wave lens. For plates whose arc lengths are less than half a circle, on the other hand, the downward convex plates are more suitable than the upward convex plates for use as lens elements. Finally for a semi-circular-arc plate, its downward convex configuration produces less reflection compared to its upward configuration in the low-frequency range, and therefore the use of these plates as lens elements depends on the frequency range of the incoming wave train. For low-frequency range

downward convex semi-circular plate is preferable while it is the opposite in the high-frequency range.

The mathematical analysis and numerical methods used here can easily be adapted, with appropriate modification, to study the reflective properties of a pair of circular-arc-shaped plates of the same or different radius submerged to the same or different depth below the free surface. Application to an elliptic arc shaped plate is also straightforward.

Acknowledgement

The authors thank the referees and Professor S. Kida, the Editor-in-chief for their comments and suggestions to revise the paper in the present form. This work is partially supported by the Council of Scientific and Industrial Research, New Delhi (through a research project of BNM).

References

Burke, J.E., 1964. Scattering of surface waves on an infinitely deep fluid. J. Math. Phys. 5, 805–819.

Dean, W.R., 1945. On the reflexion of surface waves by a submerged plane barrier. Proc. Cambridge Philos. Soc. 41, 231–238.

Dean, W.R., 1948. On the reflexion of surface waves by a submerged circular cylinder. Proc. Cambridge Philos. Soc. 44, 483–491.

Evans, D.V., 1970. Diffraction of water waves by a submerged vertical plate. J. Fluid Mech. 40, 433–451.

Heins, A.E., 1950. Water waves over a channel of finite depth with a submerged plane barrier. Canad. J. Math. 2, 210–222.

John, F., 1948. Waves in the presence of an inclined barrier. Comm. Pure Appl. Math. 1, 149–200.

Kanoria, M., Dolai, D.P., Mandal, B.N., 1999. Water wave scattering by thick vertical barriers. J. Eng. Math. 35, 361–384.

Mandal, B.N., Chakrabarti, A., 2000. Water Wave Scattering by Barriers. WIT Press, Southampton, UK.

Mandal, B.N., Dolai, D.P., 1994. Oblique water wave diffraction by thin vertical barriers in water of uniform finite depth. Appl. Ocean Res. 16, 195–203.

McIver, M., 1985. Diffraction of water waves by a moored horizontal flat plate. J. Eng. Math. 19, 297–319.

McIver, M., Urka, U., 1995. Wave scattering by circular-arc shaped plates. J. Eng. Math. 29, 575–589.

Parsons, N.F., Martin, P.A., 1992. Scattering of water waves by submerged plates using hypersingular integral equations. Appl. Ocean Res. 14, 313–321.

Parsons, N.F., Martin, P.A., 1994. Scattering of water waves by submerged curved plates and by surface piercing flat plates. Appl. Ocean Res. 16, 129–139.

Porter, D., 1972. The transmission of surface waves through a gap in a vertical barrier. Proc. Cambridge Philos. Soc. 71, 411–421.

Porter, R., Evans, D.V., 1995. Complementary approximations to wave scattering by vertical barriers. J. Fluid Mech. 294, 155–180.

Ursell, F., 1947. The effect of a fixed vertical barrier on surface waves in deep water. Proc. Cambridge Philos. Soc. 43, 374–382.

Ursell, F., 1950. Surface waves on deep water in the presence of a submerged cylinder. Part 1. Proc. Cambridge Philos. Soc. 46, 141–152.

Yu, Y.S., Ursell, F., 1961. Surface waves generated by an oscillating circular cylinder on water of finite depth: theory and experiments. J. Fluid Mech. 11, 529–551.